Environmental factors associated with long-term changes in chlorophyll-a concentration in the Amazon floodplain

Enner Alcântara[1], Evlyn Moraes Novo[1], José Stech[1], Claudio Faria Barbosa[2], Marie Paule Bonnet[3]

[1]Brazilian Institute for Space Research, Remote Sensing Division. São José dos Campos, SP – Brazil. E-mails: enner@dsr.inpe.br; evlyn@dsr.inpe.br; stech@dsr.inpe.br.
[2]Brazilian Institute for Space Research, Imaging Processing Division. São José dos Campos, SP – Brazil. E-mail: claudio@dpi.inpe.br
[3]Institut de Recherche pour le Développement. E-mail: marie-paule.bonnet@ird.fr

Abstract

The study of chlorophyll-*a* concentration in flood pulsed wetlands has been based mostly on datasets obtained at different sites or along track lines occupied during cruises. In situ water data, however, are limited in time and space. This is a particularly serious constrain in remote regions of difficult access, such as the Brazilian Amazon floodplain waters. Moreover, in situ sampling monitoring has a high probability of undersampling. Some authors have used satellite imagery to address the wide range of spatial and temporal variability of chlorophyll-a concentration in the Brazilian Amazon floodplain. However, the authors have estimated the chlorophyll concentration in a synoptic view. Also, they don't explain the relationship between the chlorophyll concentration and other environmental parameters that might explain the reported time and space variability. Long-term environmental time series of continuously collected data are fundamental to identify and classify pulses and determining their role in aquatic systems. Based on this, this paper with the objective of analyze the chlorophyll-a concentration time series and their relationship with others environmental parameters uses in situ daily mean collected limnological (chlorophyll-a concentration, water level, water surface temperature, pH and turbidity) and meteorological (wind intensity, relative humidity and short wave radiation) through an automatic system (Integrated System for Environmental Monitoring-SIMA). SIMA is a set of hardware and software designed for data acquisition and real time monitoring of hydrological systems. The data are collected in preprogrammed time interval (1 hour) and are transmitted by satellite in quasi-real time for any user in a range of 2500 km from the acquisition point. We used Pearson correlation to determine the quantitative relation between chlorophyll time series and others environmental parameters. The periods of high

variability will be studied using the Fourier power spectrum and the time-frequency structure of chlorophyll time series will be analyzed using the wavelet power spectrum. To show the relationship between chlorophyll and the significantly time series highlighted by Pearson's correlation the cross wavelet analysis was carried out and the coherence and phase analyzed. The time series of chlorophyll-a shows two high peaks (47 μg/L and 53.30 μg/L) of concentration during a year: first during the rising water and second during the low water level. A little peak was observed during the high water level (10 μg/L). For the most part of rising, high and falling water level, the chlorophyll concentration is often low (from 2.26 μg/L to 9.11 μg/L). The causes of this were discussed. The relationship between the chlorophyll-a time series and others parameters were analyzed using the Cross Wavelet and coherence and phase concepts. With periodicities ranging from 2-60 days the chlorophyll-a concentration well agrees with turbidity and water level; and coherence ~1 and in-phase for rising and low water period. Water level dynamics and turbidity explain 68% of the chlorophyll-a time series variability.

Keywords: Time series analysis, Amazon floodplain, Limnology

Introduction

In addition to its importance in photosynthesis, chlorophyll *a* is probably the most-often used estimator of algal biomass in inland waters (Wetzel, 2001) and also one of the easiest measured. The study of chlorophyll-a concentration in most of the aquatic environments has been based primarily on datasets obtained at different sites or along track lines occupied during cruises (Jerosch et al. 2006).

In situ water data measurements, however, are time and space limited. In situ time series of limnological variables are scarce. This is a particularly serious constrain in remote regions of difficult access, such as the Brazilian Amazon floodplain waters. Moreover, in situ sampling monitoring has a high probability of undersampling (Alcântara et al. 2009).

Some authors have used satellite imagery to address the wide range of spatial and temporal variability of chlorophyll-a concentration in the Brazilian Amazon floodplain (Novo et al. 2006). However, the authors have estimated the chlorophyll concentration in a synoptic view. Also, those studies do not explore the relationship between the chlorophyll

concentration and other environmental parameters that might explain the reported time and space variability.

Additionally, long-term environmental time series of continuously collected data are fundamental to identify and classify pulses and determine their role in aquatic systems (Tundisi et al. 2004). These pulses can be natural or induced for antropic activity, frequent, seasonal or intermittent, with variable magnitude and both direct and indirect effect.

Based on this, our main objective is to study the temporal variability of chlorophyll-a concentration and the controlling environmental parameters in a Brazilian Amazon floodplain, called Curuai.

Study Site and Background

This floodplain, located 850 km from the Atlantic Ocean (Figure 1), near Óbidos city (Pará State, Brazil), is formed by 'white' water lakes characterized by high concentration of suspended sediments, 'black' water lakes with high concentration of dissolved organic matter and low concentration of sediments and 'clear' water lakes fed by rainfall and rivers draining from the surrounding 'Terra Firme' (Novo et al. 2006; Melack, 1984; Engle and Sarnelle, 1990; Martinez and Le-Toan, 2006). During rising water, sediment-rich river water (white water) inundates the floodplain and directly enters many of the lakes (Forsberg, 1988). During low water, when the lakes are shallower and often isolated from mainstem influence, sediment resuspension can also produce high levels of inorganic turbidity (Junk, 1997).

Based on data acquired from 2001-2002, Bonnet et al., 2008 showed that Curuai lake is filled by water of different sources. In early January (over the course of the 2001–2002 water year), the Amazon River dominated the mixture (64%). From this date until the beginning of April, the river water contribution slightly decreased while contributions from watersheds and direct rainfall increased. By mid-April water from rainfall constituted as much as 17% while contributions from local upland watershed and from watershed located in the aquatic-terrestrial transition zone reached their maxima by the end of February, constituted 14% and 15%, respectively. The groundwater reservoir contribution was highest at the end of December reaching 5% of the mixture (Bonnet et al. 2008).

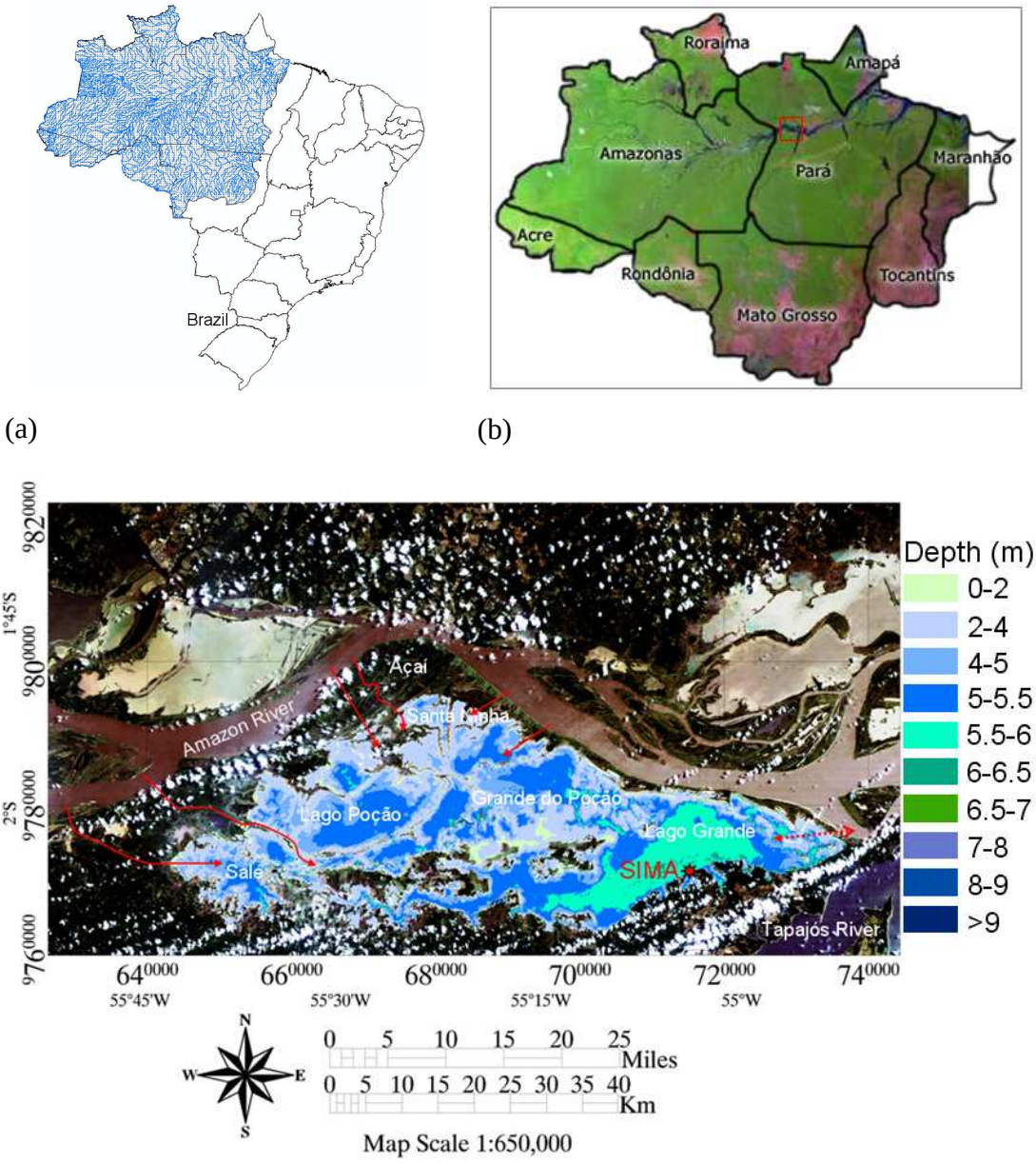

Figure 1: (a) Location of Legal Amazon in Brazil, (b) Legal Amazon limits, and (c) Location of Curuai Floodplain (Pará State, Brazil) and the location of the automatic environmental data collection buoy system SIMA at 'Lago Grande'. The arrows indicate the main channels of connection Amazon River-floodplain.

The residence time of the riverine water within the floodplain is 5 ± 0.8 month, while the residence time of water from all sources is 3 ± 0.2 months (11). The lowest and highest absolute water levels recorded at the Curuaí gauging station during the 1982-2003 period were 3.03 m and 9.61 m, respectively.

Data Acquisition

The in situ data was collected from 2004 to 2007 by an autonomous system called 'SIMA' (Integrated System for Environmental Monitoring). SIMA is a set of hardware and software designed for data acquisition and real time monitoring of hydrological systems (Stech et al. 2006). Its is composed of an independent system formed by an anchored buoy, in which sensors, data storage systems, battery and the transmission antenna are fixed (Figure 2).

Figure 2: Photo of the SIMA installed at Curuai floodplain (see Figure 1 for location).

The data are collected in preprogrammed time interval (1 hour) and are transmitted by satellite in quasi-real time for any user in a range of 2500 km from the acquisition point. In this study we use the mean time series of these four years of collected data of the following environmental parameters chlorophyll-a (μgL^{-1}), turbidity (NTU), water level (m), wind intensity (ms^{-1}), relative humidity (%), short wave radiation (Wm^{-2}) water surface temperature (ºC) and pH. The characteristics of the sensors used to limnological and meteorological parameters are show in Table 1.

Table 1: Characteristics of the limnological and meteorological sensors installed at SIMA.

Sensor	Manufacture	Range	Accuracy	Depth/Height
Chlorophyll-a	Yellow Spring	0-400 μm	0.1 μm	-1.30 m
Water Temperature	Yellow Spring	-5-60 ºC	± 0.15ºC	-1.30 m
Turbidity	Yellow Spring	0-1000 NTU	0.1 NTU	-1.30 m
Wind	R.M. Young	0-100 ms^{-1}	± 0.3 ms^{-1}	3 m
Humidity	Rotronic	0-100 %	± 1.5 %	3 m
Short wave	Novalynx	0-1500 Wm^{-2}	± 5%	3 m

Data Analysis

A Pearson correlation was run to determine the quantitative relation between chlorophyll time series and others environmental parameters (Zar, 1996). The periods of high variability were studied using the Fourier power spectrum (Bloomfield, 2000; Press, 1992) and the time-frequency structure of chlorophyll time series was analyzed using the wavelet power spectrum (Torrence and Compo, 1998). To show the relationship between chlorophyll and the significantly time series highlighted by Pearson's correlation the cross wavelet analysis was carried out and the coherence and phase analyzed (Grinsted, 2004).

The time frequency space of chlorophyll-a time series was analyzed using the wavelet transform. Wavelet analysis is becoming a common tool for analyzing localized variations of power within an environmental time series (Meyers, 1993). Decomposing an environmental time series into time-frequency space allows for the determination of both the dominant modes of variability and how those modes vary in time. We analyzed the chlorophyll-a time series obtained from SIMA data by continuous wavelet analysis using the Morlet wavelet as reference analyzing function (the so-called "mother wavelet", Farge, 1992).

To explain in more detail the importance of wind on chlorophyll-a time series evidenced by (Alcântara et al. 2008) and (Alcântara et al. 2009) we apply the cross wavelet and wavelet coherence in these two time series (Maraun and Kurths, 2004). The calculation procedures of cross wavelet and wavelet coherence were coded in Matlab 6.5 (The MathWorks, Inc., Natick, MA).

Results

A general analysis of the chlorophyll-a concentration time series shows two highlighted peaks: the first during January-February and the second during October-November while concentration remains low from March-September and in December (Figure 3). The turbidity time series has a great peak from October to November, a small peak from January to February and remains relatively low all the rest of the year except a peak in August. Note that chlorophyll concentration and turbidity time series have quasi-same peaks and that these peaks occur during rising and low water level. The wind intensity is higher from March to August than September-November.

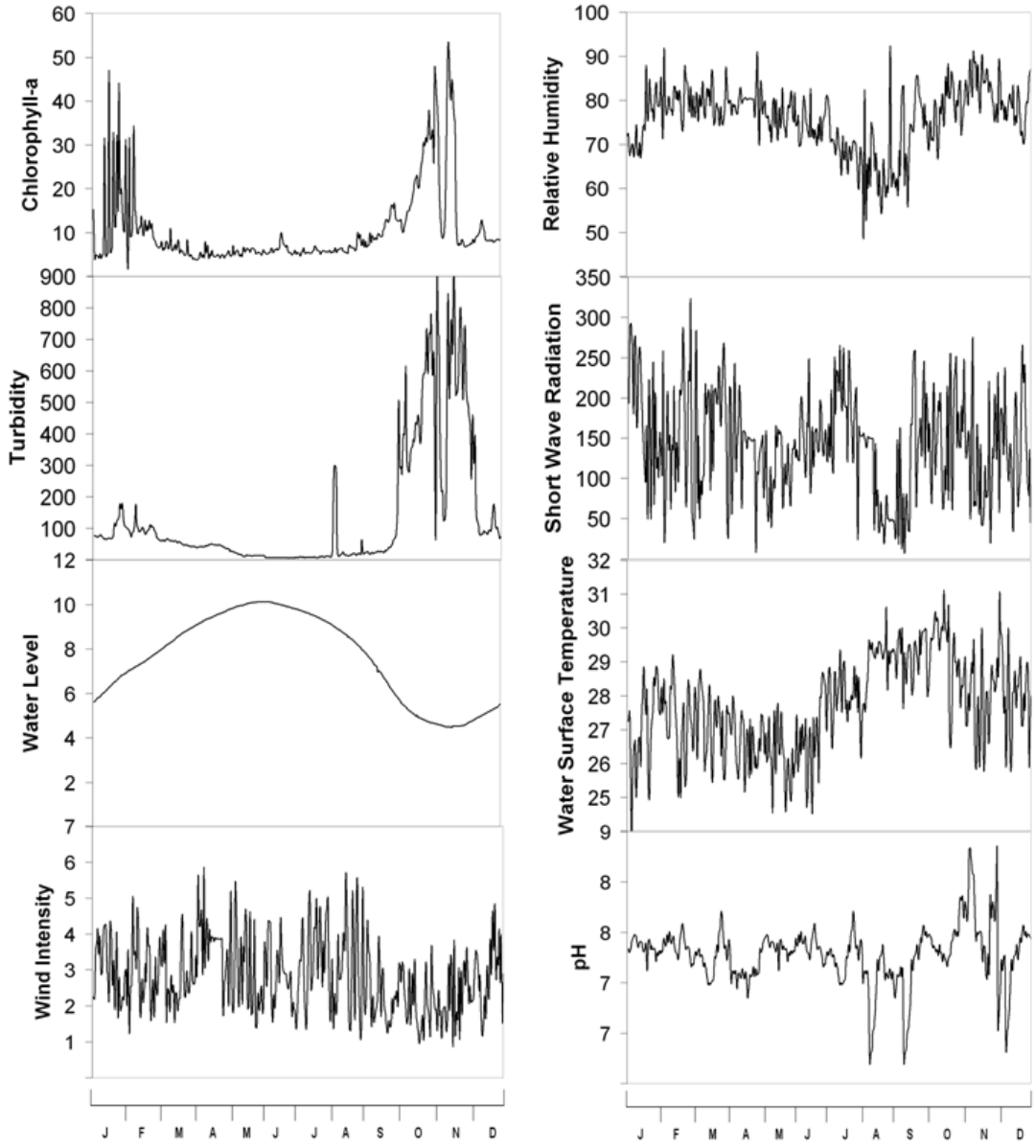

Figure 3: Time series of limnological and meteorological variables measured by SIMA.

The relative humidity has two peaks, first in the beginning of the time series and second in the end; also a decrease in August-September when the short wave radiation is shutting down. The pH has a relatively small variability through the time, with just some interesting events, one in August and September when the pH is below 7 and in November when the value rises until ~8.8. A descriptive statistics (maximum, minimum, mean and standard deviation) of these time series is show in Table 2.

Table 2: Descriptive statistics for the time series: Chlorophyll-a (*Chl*), water level (*WL*), wind intensity (*WI*), relative humidity (*Rh*), short wave radiation (*SW*), water surface temperature (*WST*), pH and turbidity (*Tur*).

Variables	Max	Min	Mean	SD
Chl	53.30	2.26	10.45	± 9.11
Tur	913.24	5.76	133.93	± 198.92
WL	10.13	4.45	7.60	± 1.95
WI	5.86	0.86	2.83	± 1.04
Rh	92.31	49.02	75.95	± 7.26
SW	319.30	8.33	142.16	± 64.95
pH	8.34	6.20	7.28	± 0.29
WST	31.12	23.73	27.72	± 1.40

The time series of chlorophyll-a was adjusted using eight Gaussian-terms. Due to the high variability observed by the end of January and by October-November (Figure 4-a) the model did not capture all the variability. This is observed in Figure 4-b which shows the highest residuals during this period. From August to May and July to September the model worked very well. The overall fitting was R^2=0.94 ($p = 0.05$ and $RMSE = 1.96$). This pattern of variability will be analyzed by Fourier and wavelet analysis.

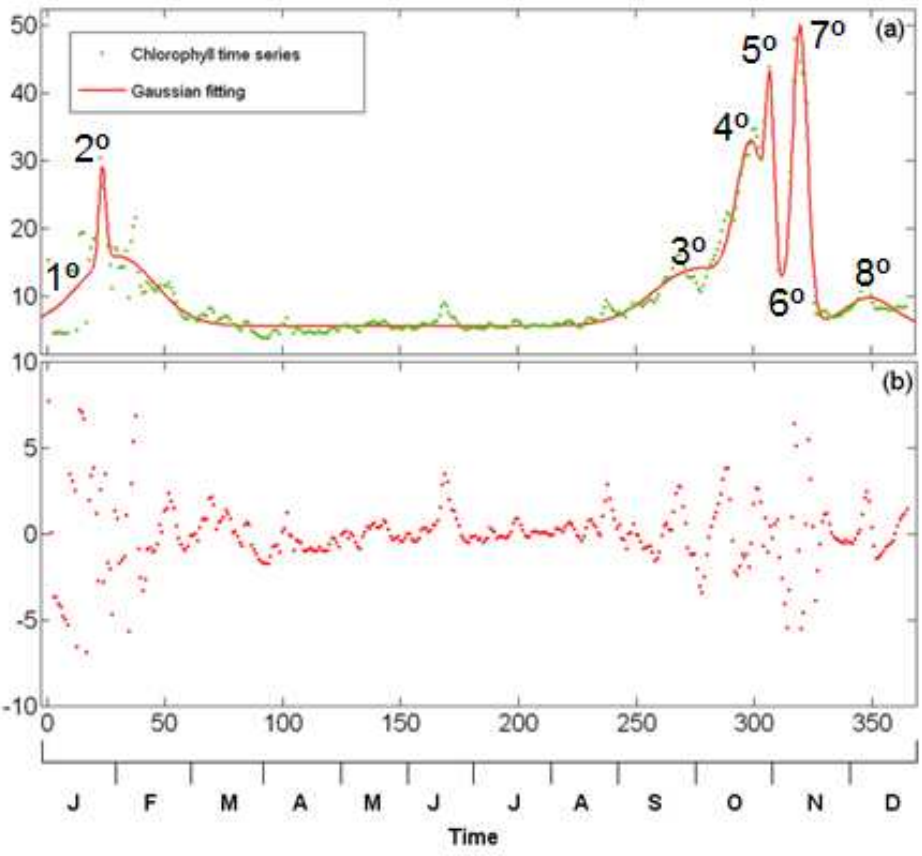

Figure 4: Fitting the chlorophyll-a time series using eight-term Gaussian series.

The mathematical representation of this Gaussian fitting could be represented as:

$$f(t) = \overbrace{14.13}^{h} \exp\left(-\left(\frac{t-\overbrace{23.61}^{\mu}}{\underbrace{2.03}_{\sigma}}\right)^2\right) + 10.29\exp\left(-\left(\frac{t-29.96}{22.69}\right)^2\right) + 8.45\exp\left(-\left(\frac{t-276.5}{26.29}\right)^2\right) +$$
$$23.41\exp\left(-\left(\frac{t-299.5}{9.16}\right)^2\right) + 23.69\exp\left(-\left(\frac{t-307.3}{2.47}\right)^2\right) + 13.37\exp\left(-\left(\frac{t-(-1.06\text{x}10^6)}{1.41\text{x}10^6}\right)^2\right) + \quad (1)$$
$$43.67\exp\left(-\left(\frac{t-319.9}{4.42}\right)^2\right) + 4.19\exp\left(-\left(\frac{t-349.4}{14.74}\right)^2\right)$$

Where (h) is the amplitude, (t) time, (μ) the central or peak position and (σ) the variance.

The first Gaussian-term represents the variability of the chlorophyll-a concentration in January with a standard deviation of 2.03 (μgL^{-1}), that was the smallest value of the whole

series. The second with a standard deviation of 22.69 (μgL^{-1}) is representative of the beginning of February until the end of August. The third represents the variability from beginning of September to beginning of October. The forty Gaussian terms is related from beginning to middle of October. Fifth Gaussian term represents the variability from middle to the end of October. Sixth presents the Gaussian model for beginning of November and it is the unique Gaussian term that was negative; these occur due to a high decrease of the concentration during the transition of October-November. Seventh Gaussian presents a mathematical representation of the variability from beginning to the end of November. And finally the eighth represents the chlorophyll variability from the beginning to the end of December of the time series. All this variability could be addressed using the Fourier analysis.

The Fourier power spectrum applied on chlorophyll-a time series shows that the power density increases with time with four major peaks, the first in 6 days, second in 18 days, the third in 30 days and in 46 days (Figure 5). Also we observe a continuously increasing power density in 55 days.

The period of 6 days is associated with so called pulse that was presented above. This means that in short periods of days the chlorophyll-a change rapidly and stay associated with the two major peaks (beginning of January and October-November) presented above in Figure 4. The periods of 18 days is associated, probably, with the two peaks presented in Figure 4 from October-November. Periods higher than 30 days are associated with relatively small peaks in half of June and the end of November. For a more detailed evaluation about these periods a wavelet transform was run.

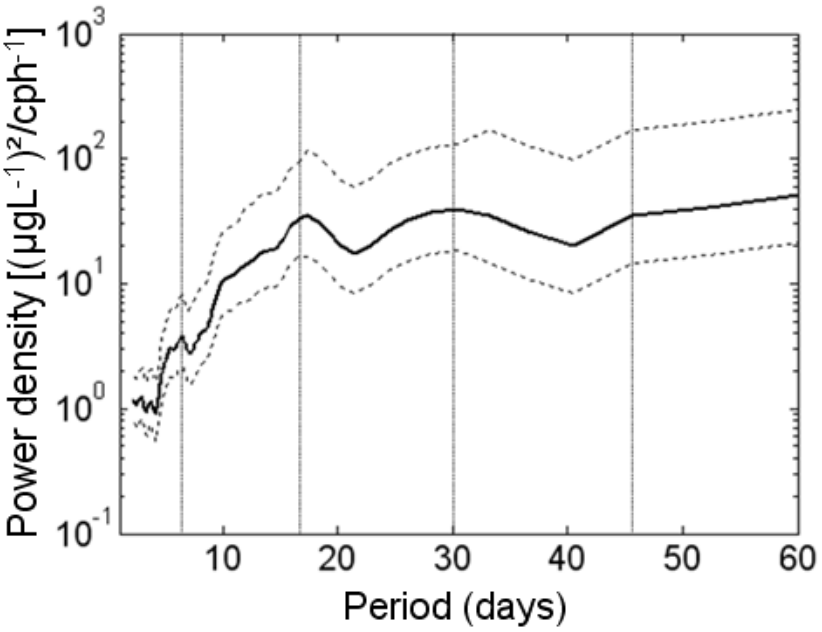

Figure 5: Fourier power spectrum of chlorophyll-a time series. The dashed lines represent the confidence intervals limits.

The wavelet power spectrum show in Figure 6 reveals that the significant periods is high in the half of December and January (D-J) of the time series and low from February to July (F-J) and tends to increase again from August to November (A-N). The most powerful periods is related to 2-32 days band for D-J, 16-128 days band for F-J and 2-64 days band for A-N.

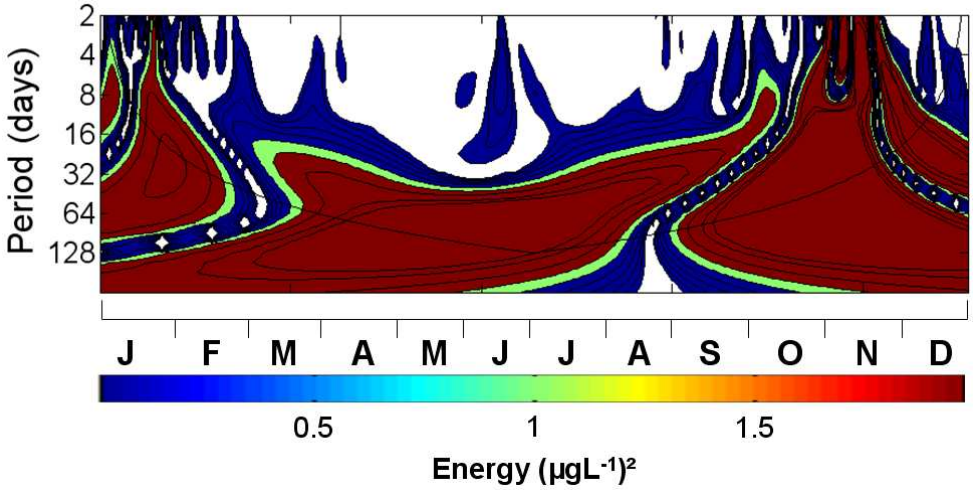

Figure 6: Wavelet analysis of chlorophyll-a concentration time series. The line cross the power spectrum indicates the “cone of influence,” where edge effects become important.

The influence of others environmental parameters on chlorophyll-a annual variability pattern will be checked; first using the Pearson's correlation.

Pearson's Correlation

The results of Pearson's correlation (Table 2) shows that the chlorophyll-a time series is negatively correlated with water level (-0.57) and positively with turbidity (0.66). That means, when we have an increase of water level the chlorophyll concentration decrease and when chlorophyll concentration increases the turbidity increases. The others parameters show a low correlation and then we will consider just the mentioned variables to try to explain the chlorophyll-a variability. The short wave radiation and pH does not show significant correlation with chlorophyll-a concentration and will not be used to explain the chlorophyll variability.

Table 2: Pearson correlation coefficients for Chlorophyll-a (*Chla*) against water level (*WL*), wind intensity (*WI*), relative humidity (*Rh*), short wave radiation (*SW*), water surface temperature (*WST*), pH and turbidity (*Tur*).

Variables	$\mathbf{R^2}$
Tur	0.66
WL	-0.57
Rh	0.26
WI	-0.26
WST	-0.16
SW	-
pH	-

Only significant values at 95% significance level are shown.

Seasonal variability of shortwave radiation is very low in the study area compared with other regions of the world. Changes in incoming shortwave radiation are not directly a driving factor for photosynthesis or communities successions, but probably light availability does as mentioned by (Forsberg, 1988). The floodplain alkalinity is relatively medium when compared with the average of world rivers (Martin and Meybeck, 1979),

strong primary production and/or respiration activities should therefore lead to significant pH changes during the day but daily-averaged values do not allow studying this.

The water level dynamics and turbidity explain 68% of the chlorophyll-a time series variability (RMS=11.27 µg/L, $\rho = 0.04$) and could be represented as:

$$Chl = 23.01 + (-0.20\mathrm{WL}) + (-0.50\mathrm{Tur}) \quad (2)$$

The time frequency structure between chlorophyll and turbidity and water level will be analyzed in more detail using the cross wavelet spectrum and coherence and phase. Taking into account that only water level and turbidity showed significant correlations with chlorophyll, from now on, the cross correlation analyses will be focused upon them.

Cross wavelet and coherence and phase

Cross wavelet power reveals areas with high common power between tow parameters and coherence is a measure of the correlation between two time series, at each frequency. Arrows pointing to the right mean correlation (in phase) and an anticorrelation (in antiphase) is indicated by a left pointing arrow. Non-horizontal arrows refer to a more complicated (non-linear) phase difference (Valdés-Galicia and Velasco, 2008).

The cross wavelet spectrum between chlorophyll and turbidity (Figure 9-a) is stronger from 2 to 30 days band and the same band period occurs in the beginning of the time series but with medium power. This might be explained by the fact that during the rising water level the nutrients come from upland. The coherence (Figure 9-b) is more highlighted from 3 to 50-days band (in-phase) in the beginning of the time series and from 2 to 16-days band periods (in-phase) in the end of the time series. Moreover the coherence is stronger for 32-days in the beginning and 16-days and periods for the end of time series.

For chlorophyll-a and water level the cross wavelet spectrum (Figure 9-c) shows a significant period 64-94 days band (in-phase). For periods smaller than 64 days the water level is not a determinant variable to cause algal bloom. However from September to February the water level is very important. The coherence (Figure 9-d) shows an increase of period for high coherence. That suggests that from September to December the water level dynamics is more important than from January to February.

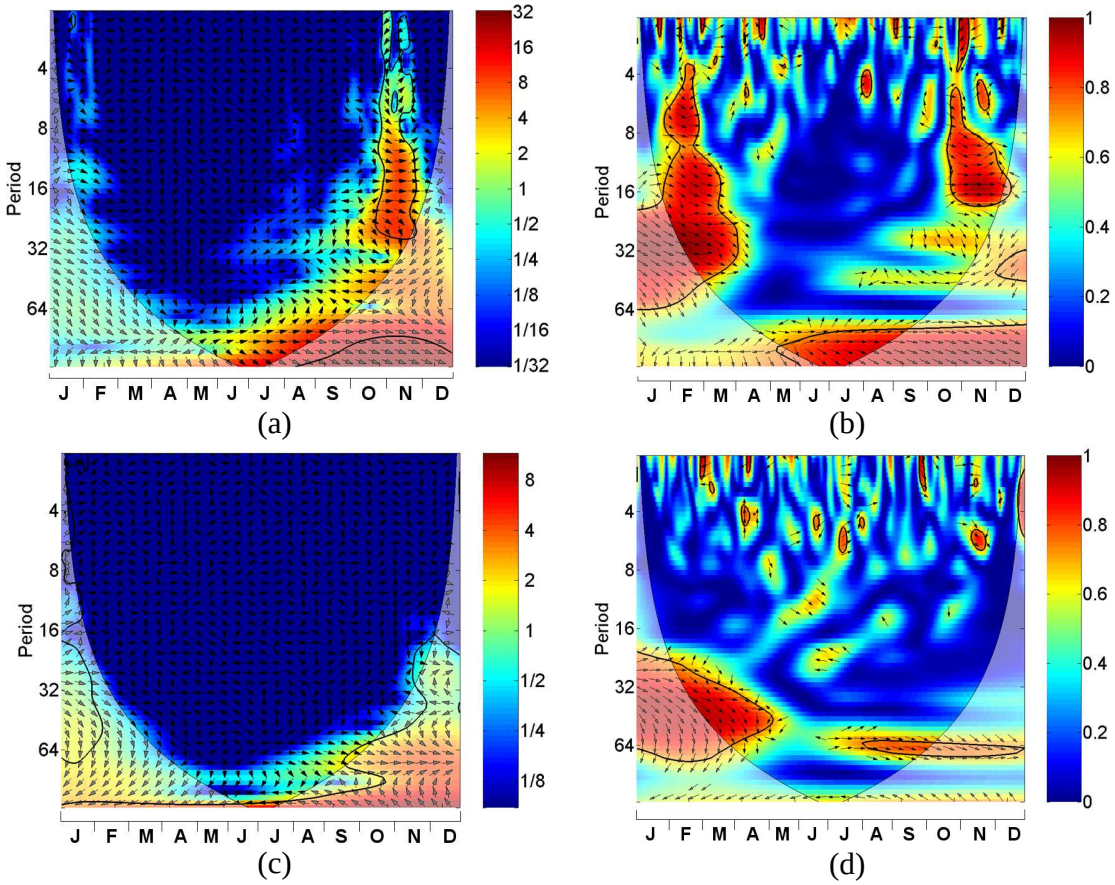

Figure 9: Cross wavelet transform of the standardized chlorophyll against turbidity (a) and water level (c). The 5% significance level against red noise is shown as a thick contour. The relative phase relationship is shown as arrows; squared wavelet coherence between the standardized chlorophyll and turbidity (b), water level (d). The 5% significance level against red noise is shown as a thick contour.

Discussion

Chlorophyll-a time series

The chlorophyll-a time series exhibits two very significant peaks, the first one occurring during January and February (rising period) and the second during low water stage (October-November). A smaller peak is also observed in June. During these peaks chlorophyll-a concentration is highly variable and can not be approximated through Gaussian series as shown in Figure 4-b. Fourier power spectrum enables to distinguish four major peaks of respectively 6, 18, 30 and 46 days while the wavelet power spectrum enabled to enlighten the more powerful periods which are: 2-32 days band for D-J, 16-128 days band for F-J and 2-64 days band for A-N.

Short-time responses are associated with the most significant peaks of chlorophyll-a and in particular the shortest time response seems to occur during October and November.. The so small periods of variability evidenced by Fourier and Wavelet is due mainly by sediment resuspension events during low water level that allow also the nutrient availability.

Controlling factors of primary production in the floodplain

In order to relate chlorophyll-a variations with environmental factors, Pearson's correlation and cross wavelet analysis were performed. Significant Pearson's correlation between water level (negative), turbidity (positive) and chlorophyll-a were obtained. Cross wavelet analysis and coherence study enabled to show a strong influence of water level during the second peak as well as a strong influence of turbidity on short-time responses while during the first peak both water level and turbidity are less significant.

Water level control on primary production

As indicated in Table 1, the water level is about two times greater during high water level stage than during low water stage and consequently the floodplain volume are varying of about a factor 3. Part of the inverse correlation obtained may therefore be attributed to chlorophyll-a dilution.

A negative correlation between water level and chlorophyll-a is also expected in turbid environments where phytoplankton has to remain in the euphotic zone. Most of the phytoplankton species tends to sediment and cells are passively transported. The stay-duration in the euphotic zone depends on the water circulation, in particular circular movement such as wave-induced currents or vertical movements that help the cells maintaining in the upper part of the water column.

When depth increases, phytoplankton has therefore less chance to maintain in the euphotic zone as reported by (Junk, 1997). However, this control depends on phytoplankton species. In the floodplain occasional blooms of cyanobacteria can occur during part of the year and these species have buoyancy control abilities that help them to remain at the surface (Uherkovich and Schmidt, 1974; Fiore et al, 2005).

As pointed out by Melack and Forsberg (2001) the total daily phytoplankton production can vary considerably in Amazon floodplain lakes due to large seasonal changes in surface area linked to water-level variations.

Turbidity control on primary production

The positive correlation between turbidity and chlorophyll-a and a high pH value found during the largest peak in O-N confirms that there is a strong production during that period of time while turbidity is high.

The short-time response observed in D-J and A-N (Figure 6) is related to higher values of chlorophyll-a concentration observed in Figure 4-a. During the peak observed in A-N when the water level is low the sediment ressuspension events can occur, as reported by (Alcântara et al. 2009). When this event occurs we have a returning of nutrients to the water column, as reported by (Forsberg et al. 1988) and supported by (Engle and Sarnelle, 1990; Carpenter, Ludwig and Brock, 1999).

Ibañez (1998) also reported for a central Amazonian floodplain, that during the rising and low water level phytoplankton species richness is higher than falling and high water level.

In the case of D-J is related to incoming water from Amazon River into floodplain and also by local water basin due to precipitation. The average annual precipitation in the Curuai floodplain is 2447 mm $year^{-1}$, compared to average potential evaporation of 1400 mm $year^{-1}$ (average obtained by a time series from 1990 to 2001), with the wet season lasting from January to June and a drier season from July to December (Barroux, 2006).

During the high water level sediment accumulates in the floodplain, while during the falling water stage it is exported to the mainstream. The mean average sediment storage calculated for the floodplain varies between 558 and 828x10^3 t yr^{-1} (Maurice-Bourgoin et al. 2007). According to (Moreira-Turcq et al. 2004) the Curuai floodplain is a sediment accumulation system, with high rate of bottom deposition in some specific lakes (i.e. Santa Ninha Lake, 1 cm yr^{-1}). Of the influx of suspended material from the Amazon River into the floodplain, about 50% is deposited. Amorim (2006) shows that in general manner the suspended materials in the Curuai floodplain is composed mainly of silt and clay.

Probably, because of this during the high and failing water level the concentration of chlorophyll-a in the Curuai floodplain is low. However, note that in June a short increasing

in chlorophyll concentration occur. This is an effect of sediment deposition and consequently light increase availability; afterward, the concentration stabilizes. This is supported by (Forsberg et al. 1988) who have found that during the high water level stage the phytoplankton growth due to high transparency caused by particulate settling.

Then a high phytoplankton growth causes a peak of chlorophyll concentration as shown in Figure 4 and it is confirmed by high pH values (around 8.8) indicating a strong photosynthesis activity. Immediately afterwards a decrease of chlorophyll concentration occurs. This decrease was captured by the Sixth Gaussian term of the Equation 1. With high turbidity and high competition for nutrients and solar radiation some cells starts to die, increasing the concentration of dissolved organic matter and decreasing of dissolved oxygen, as shown by (Barbosa, 2005).

Summary and Conclusion

The present works is a contribution to understanding the chlorophyll variability through the time. In summary, we have demonstrated that:

- A general analysis of the chlorophyll-a concentration time series shows two highlighted peaks: first during January-February and second during October-November while concentration remains low from March-September and in December;
- Chlorophyll concentration and turbidity time series have quasi-same peaks and that these peaks occur during rising and low water level;
- An abrupt decay of the chlorophyll concentration occur during the transition of October-November;
- The chlorophyll-a time series was correlated with water level (negatively) and turbidity (positively);
- Short wave radiation and pH was no correlated at 95% of significance;
- For periods smaller than 64 days the water level is not a determinant variable to cause algal bloom. However from September to February the water level is very important;

So we conclude that the primary driven force for influencing the chlorophyll-a concentration through the time in Curuai floodplain is the turbidity and the water level dynamics. As a secondary are short wave radiation and pH.

Acknowledgements

The authors are grateful to the Brazilian funding agency FAPESP under grants 02/09911-1 and the Brazilian Council for Science and Technology (Grant CNPq- CTHIDRO – 55.0301/02-0, Grant CNPq n.º 477885/2007-1). Evlyn Novo thanks CNPq grant 304929/2007 and Enner Alcântara CAPES grant 0258059 and FAPESP 2007/08103-2. We also thank C. Torrence and G. Compo for provides the Wavelet software available at URL:http://atoc.colorado.edu/research/wavelets/ and to A. Gristed for provides the cross wavelet and wavelet coherence algorithm software available at URL: http://www.pol.ac.uk/home/research/waveletcoherence/.

References

Alcântara, E.H.; Stech, J.L.; Novo, E.M.L.M.; Shimabukuro, Y.E.; Barbosa, C.C.F. Turbidity in the Amazon floodplain assessed through a spatial regression model applied to fraction images derived from MODIS/Terra. IEEE Trans. Geo. Rem. Sens. 2008, 46 (10), 2895-2905.

Alcântara, E.H.; Barbosa, C.C.F.; Stech, J.L.; Novo, E.M.L.M.; Shimabukuro, Y.E. Improving the spectral unmixing algorithm to map water turbidity distributions. Environ. Model. & Soft. 2009, 24 (9), 1051-1061.

Alcântara, E; Novo, E.; Stech, J.; Lorenzzetti, J.; Barbosa, C.; Assireu, A.; Souza, A. The turbidity behavior in an Amazon floodplain. Hydrol. Earth Syst. Sci. Disc. 2009, 6, 3947-3992.

Amorim, M.A. Study of early sedimentation in 'Lago Grande de Curuai' várzea, Pará State, Brazil. MSc. Dissertation, Fluminense Federal University, Niterói, Brazil. 2006.

Barbosa, C.C.F. Sensoriamento remoto da dinâmica de circulação da água do sistema planície de Curuai/ Rio Amazonas. PhD. Dissertation, National Institute for Space Research, São José dos Campos, Brazil. 2005.

Barroux, G. Bio-geochemical study of a lake system from the Amazonian floodplain: the case of 'Lago Grande de Curuaí, Pará-Brazil PhD. Dissertation. Université Paul Sabatier, Toulouse, France. 2006.

Bloomfield, P. Fourier analysis of time series: an introduction.John Wiley & Sons: New York, 2000.

Bonnet, M.P.; Barroux, G.; Martinez, J.M.; Seyler, F.; Moreira-Turcq, P.; Cochonneau, G.; Melack, J.M.; Boaventura, G.; Maurice-Bourgoin, L.; León, J.G.; Roux, E.; Calmant, S.; Kosuth, P.; Guyot, J.L.; Seyler, P. Floodplain hydrology in an Amazon floodplain lake (Lago Grande de Curuaí). J. Hydrology. 2008, 349 (1-2), 18-30.

Carpenter, S.R.; Ludwig, D.; Brock, W.A. Management of eutrophication for lakes subject to potentially irreversible change. Ecological Applications. 9(3), 751-771. 1999.

Engle, D.L.; Sarnelle, O. Algal use of sedimentary phosphorus from an Amazon floodplain lake: implications for total phosphorus analysis in turbid waters. Limnol. Oceanogr.1990, 35 (2), 483-490.

Farge, M. Wavelet transforms and their applications to turbulence. Ann. Rev. Fluid Mech. 1992, 24 (1), 395-457.

Fiori, M.F.; Neilan, B.A.; Copp, J.N.; Rodrigues, J.L.M.; Tsai, S.M.; Lee, H.; Trevors, J.T. Characterization of nitrogen-fixing cyanobacteria in the Brazilian Amazon floodplain. Water Research 39: 5017-5026. 2005.

Forsberg, B. R.; Devol, A. H.; Richey, J. E.; Martinelli, L. A.; Des Santos, H. Factors controlling nutrient concentrations in Amazon floodplain lakes. Limnol. Oceanogr. 1988, 33 (1) 41-56.

Grinsted, A.; Moore, J.C.; Jevrejeva, S. Application of the cross wavelet transform and wavelet coherence to geophysical time series. Non. Lin. Proc. Geophy. 2004, 11 (5-6), 561-566.

Ibãnez, M.S.R. Phytoplankton composition and abundance of a central Amazonian floodplain lake. Hydrobiologia. 1998. 362:79-83.

Jerosch, K.; Schlüter, M.; Pesch, R. Spatial analysis of marine categories information using indicator Kriging applied to georeferenced video mosaics of the deep-sea Håkon Mosby Mud Volcano. Ecol. Infor. 2006, 1 (4), 391-406.

Junk, W.J. The Central Amazon Floodplain: ecology of a pulsing system, 1rd Ed.; Springer Verlag: Berlin, Germany. 1997.

Martin, J.M.; Meybeck, M. Elemental mass balance of material carried by major world rivers. Marine Chemistry. 7: 173-206. 1979.

Martinez, J-M.; Le-Toan, T. Mapping of flood dynamics and spatial distribution of vegetation in the Amazon floodplain using multitemporal SAR data. Rem. Sens. Envir. 2006, 108 (3), 209-223.

Maurice-Bourgoin, L.; Bonnet, M.P.; Martinez, J.M.; Kosuth, P.; Cochonneau, G.; Moreira-Turcq, P.; Guyot, J.L.; Vauchel, P.; Filizola, N.; Seyler, P. Temporal dynamics of

water and sediment exchanges between the Curuaí floodplain and the Amazon River, Brazil. J. Hydrology. 2007, 335 (1-2), 140-156.

Maraun, D.; Kurths, J. Cross wavelet analysis: significance testing and pitfalls. Non. Lin. Proc. Geophy. 2004, 11 (5-6) 505-514.

Meyers, S.D.; Kelly, B.G.; O'Brien, J.J. An introduction to wavelet analysis in Oceanography and Meteorology: with application to the dispersion of Yanai Waves. Mon. Wea. Rev. 1993, 121 (10), 2858-2866.

Melack, J.M. Amazon floodplain lakes: shape, fetch and stratification. Int. Ver. Theor. Angew. Limnol. Verh. 1984, 22, 1278-1282.

Melack, J.M.; Forsberg, B.R. Biogechemistry of Amazon floodplain lakes and associated wetlands. In: McCalin, M.E.; Victoria, R.L.; Richey, J.E. (Eds) The biogeochemistry of the Amazon basin. Oxford University Press. Cap. 14, pp. 235-274. 2001,

Moreira-Turcq, P.F.; Jouanneau, B.; Turcq, B.; Seyler, P.; Weber, O.; Guyot, J.L. Carbon sedimentation at Lago Grande de Curuaí, a floodplain lake in the low Amazon region: insight into sedimentation rates. Palae. Palae. Palae. 2004, 214 (1-2), 27-70.

Novo, E.L.M.M.; Barbosa, C.C.F.; Freitas, R.M.; Shimabukuro, Y.E.; Melack, J.M.; Pereira-Filho, W. Seasonal changes in chlorophyll distribution in Amazon floodplain lakes derived from MODIS images. Limnology. 2006, 7 (3), 153-161.

Press, W.H.; Teukolsky, S.A.; Vetterling, W.T.; Flannery, B.P. Numerical recipes in fortran 77: the art of scientific computing. V.1 of Fortran numerical recipes. Cambridge University Press: UK. 1992.

Stech, J.L.; Lima, I.B.T.; Novo, E.M.L.M.; Silva, C.M.; Assireu, A.T.; Lorenzzetti, J.A.; Carvalho, J.C.; Barbosa, C.C.F.; Rosa, R.R. Telemetric monitoring system for meteorological and limnological data acquisition. Verh. Internat. Verein, Limnol. 2006, 29, 1747-1750.

Torrence, C.; Compo, G.P. A Practical Guide to Wavelet Analysis. Bull. Amer. Meteor. Soc. 1998, 79, 61-78.

Tundisi, J. G.; Matsumura-Tundisi, T.; Arantes Junior, J. D.; Tundisi, J. E. M.; Manzini, N. F.; Ducrot, R. The response of Carlos Botelho (Lobo, Broa) reservoir to the passage of cold fronts as reflected by physical, chemical and biological variables. *Braz. J. Bio*. 2004, 64 (1) 177-186.

Valdés-Galicia, J.F.; Velasco, V.M. Variations of mid-term periodicities in solar activity physical phenomena. Advances in Space Research. 41, 297-305, 2008.

Wetzel, R.G. Limnology – Lake and River Ecosystems, 3rd Ed.; Academic Press: San Diego, USA. pp. 1006, 2001.